JOURNAL OF Materials CHEMISTRY

# Synthesis and dielectric characterisation of lead magnesium niobate from precipitation and freeze-drying methods

**W. B. Ng,[a] J. Wang,*[a] S. C. Ng[b] and L. M. Gan[c]**

[a]*Department of Materials Science,* [b]*Department of Physics,* [c]*Department of Chemistry/IMRE, National University of Singapore, Singapore 119260*

***Received 11th June 1998, Accepted 1st July 1998***

Lead magnesium niobate, $Pb(Mg_{1/3}Nb_{2/3})O_3$ (PMN), has been prepared from aqueous nitrate solutions by freeze-drying and stepwise precipitation using an ammonia solution as the precipitant. Perovskite PMN powders with less than 5% pyrochlore phase were obtained when the resulting precursors were calcined at temperatures in the range of 800 to 1000 °C. They exhibited a rounded powder morphology and an average agglomerate size of $<1.0$ μm. Freeze-dried PMN offered a lower formation temperature for the perovskite phase (700 °C) and a higher relative permittivity than those of precipitated PMN. On sintering at 1150 °C, the maximum relative permittivity observed for the precipitated PMN was 8019 at 1 kHz with a Curie temperature of −11 °C, while that of freeze-dried PMN was 14542 with a Curie temperature of −3 °C at the same frequency.

## Introduction

Lead magnesium niobate, $Pb(Mg_{1/3}Nb_{2/3})O_3$ (PMN), has been extensively studied as a relaxor ferroelectric material due to its wide applications in the field of multilayer capacitors (MLC), actuators and many other electronic devices. It offers excellent electrical properties including high relative permittivity ($\varepsilon>12000$ at 20 °C),[1–3] large electrostrictivity[2,4–7] and attractive physical properties such as low thermal expansion and diffuse-phase transition (DPT).[8,9] However the performance of PMN is often limited by the co-existence of a pyrochlore phase with the perovskite structure. Throughout the years researchers in the field of electroceramics have been studying the formation of monophasic PMN with minimal pyrochlore phase present.

In an attempt to avoid pyrochlore phase formation as well as to produce PMN powders of controlled morphologies, high purity and narrow size distribution, wet chemical synthesis has evolved as a major field of research in recent years. The advantages of chemistry-based processing routes are obvious; they increase the homogeneity of resulting powders by mixing the reagents at the molecular level in solution. This is especially useful in the preparation of a multicomponent system such as PMN. The oxide powders derived from these chemistry-based processing routes have high specific surface area and, consequently, readily undergo the solid-state interaction and sintering.[10] Techniques such as coprecipitation,[11] sol–gel,[12–14] citrate route,[15,16] molten salt[17] and partial oxalate methods[18,19] are among those which have been developed. However, the success of precipitation or coprecipitation of solutes from a homogeneous solution is controlled by parameters such as solution pH, temperature, type and concentration of precipitant, hydrolysis rate of cations, *etc*.[20] The stoichiometry of a multicomponent compound may be lost when the precipitates involved exhibit very different solubility in the aqueous solution. This may be prevented in the freeze-drying technique, which has been advocated as a chemical process capable of producing pure, chemically homogeneous and above all ultrafine powders.[21] It involves the preparation of an aqueous or non-aqueous solution containing cations of interest, followed by rapid freezing of the solution and subsequent sublimation of the solvent under high vacuum. The technique was applied to produce fine ceramic powders three decades ago by Schnettler *et al.*[22] Since then it has been utilised to synthesize a wide spectrum of ceramic materials such as hematite,[23] lithium ferrite,[24] and Y–Ba–Cu–O superconductors[25] among many others. It has also been proven effective in controlling the chemical homogeneity of multicomponent electroceramic powders such as lanthanum-doped lead zirconate titanate (PLZT)[26] and PMN.[27]

In this study, PMN powders of high perovskite content were prepared *via* two chemistry-based powder preparation routes, namely freeze-drying and stepwise precipitation. To avoid the use of expensive metal alkoxides which are difficult to handle due to their moisture sensitivity, inorganic metal salts are used as starting materials for both of the processing routes. A method of preparing an aqueous solution of $Pb^{2+}$, $Mg^{2+}$ and $Nb^{5+}$ ions in the form of nitrates will be described in detail. Freeze-drying was hence carried out on the aqueous Pb–Mg–Nb nitrate solution. Secondly, PMN precursors were obtained *via* stepwise precipitation using aqueous ammonia similar to the two-step hydrolysis process devised by Yoshikawa and Uchino.[28] However the aqueous nitrate solution was used in this study instead of a peroxo-niobium complex solution. Though there have been independent studies on processing of PMN *via* freeze-drying[27] and stepwise precipitation,[28] there have been no reports on the dielectric properties of PMN ceramics fabricated from such derived powders. Hence it is the objective of this work to compare the two processes of PMN formation and the properties of the resulting powders. Powders derived from both processes were characterised and compared in terms of their thermal decomposition, phase formation and particle characteristics. Dielectric properties, such as relative permittivity and dissipation factor of sintered PMN ceramics, were also measured.

## Experimental procedure

### Preparation of PMN-nitrate solution

Niobium pentachloride $NbCl_5$ (Fluka 99.9%) was added to an excess amount of 2 M $NH_3$ (aq) to form the hydrated niobate $Nb_2O_5 \cdot xH_2O$, which was filtered off and repeatedly washed free of chloride ions when tested with silver nitrate solution. The amount of niobium content in the hydrated niobate was determined by thermogravimetric analysis based on niobium oxide ($Nb_2O_5$) as the final form. The freshly precipitated hydrated niobate was then dissolved in 1 M hot oxalic acid to yield a niobium oxalate solution.[29]

With the subsequent addition of a lead nitrate solution to the niobium oxalate solution, a white gel of lead oxalate, $Pb(C_2O_4)$, was immediately precipitated. Although lead oxa-

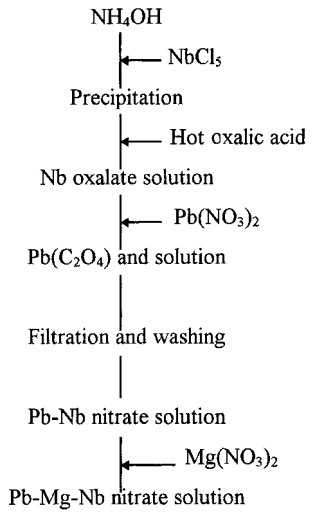


**Scheme 1** Preparation of a PMN aqueous solution.

late could be redissolved by adding concentrated nitric acid, the resulting solution was not suitable for coprecipitation using an ammonia solution as the precipitant, since lead oxalate will again be preferentially precipitated.[28] Hence a precalculated amount of lead nitrate $Pb(NO_3)_2$ (Merck >99%) dissolved in distilled water was added to the niobium oxalate solution to fully precipitate the oxalate ions as lead oxalate and with the required amount of lead ions remaining in the solution. A lead–niobium nitrate solution was thus obtained after lead oxalate was filtered off. An appropriate amount of magnesium nitrate, $Mg(NO_3)_2 \cdot 6H_2O$ (Fisons 99.0–101.0%), was then added to the lead–niobium nitrate solution, forming an aqueous PMN nitrate solution. A flow chart for the described preparation of PMN nitrate solution is shown in Scheme 1.

### Freeze-drying

The aqueous solution containing $Pb^{2+}$, $Mg^{2+}$ and $Nb^{5+}$ cations prepared as detailed above was frozen in a flask immersed in a mixture of acetone and dry ice. The frozen product was immediately adapted to a freeze dryer (Labconco, Model 77400) and freeze-drying was carried out at a vacuum of *ca.* $200 \times 10^{-3}$ mmHg (0.266 mbar) and a temperature of $-40\,^{\circ}C$ until most of the water solvent was eliminated by sublimation. The resulting precursor was dried in an oven and then kept in a sealed container as it was highly moisture-sensitive.

### Stepwise precipitation

A one-step coprecipitation of the Pb–Mg–Nb nitrate solution using either ammonia solution or NaOH solution resulted in the formation of a precursor which did not produce any perovskite phase after calcination even at 1000 °C. This was due to the fact that the resulting precursor was magnesium-deficient since magnesium hydroxide is highly soluble in the presence of nitrate ions. The same problem was encountered by other investigators.[28] Hence the stepwise precipitation method as devised by Yoshikawa and Uchino[28] was adopted. For this, a lead–niobium nitrate solution was initially prepared as described before. An appropriate amount of 2 M ammonia solution was then titrated into the solution to form lead–niobium hydroxide precipitates, followed by filtration and washing using distilled water before they were ultrasonically dispersed in a magnesium nitrate solution to form a slurry. A second precipitation was carried out by adding a desirable amount of ammonia solution into the suspension. The resulting coprecipitates were filtered off and washed repeatedly, followed by drying in the oven overnight. The procedure is depicted in Scheme 2.

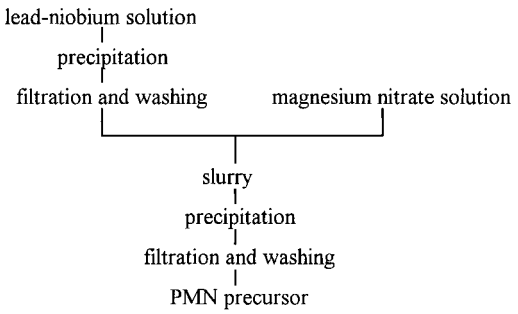


**Scheme 2** Preparation of PMN powders by stepwise precipitation.

### Precursor and powder characterization

The two precursors were investigated using thermogravimetric analysis (TGA) and differential thermal analysis (DTA) performed on a Dupont 2100 thermal analyser. Samples of 10–15 mg were heated in air at a rate of $10\,^{\circ}C\,min^{-1}$ from room temperature to 900 °C in both analyses. They were then calcined at various temperatures ranging from *ca.* 700 to 1000 °C in a closed high alumina crucible for 2 hours, followed by phase identification using X-ray diffraction (XRD, Cu-Kα, Phillips 1729). The particle size and size distribution of the resulting powders were measured using the laser light scattering technique (Horiba-LA910). The calcined powders were also characterized for particle size and morphology using a scanning electron microscope (JEOL JSM 35CX) and a transmission electron microscope (JEOL Model 100CX).

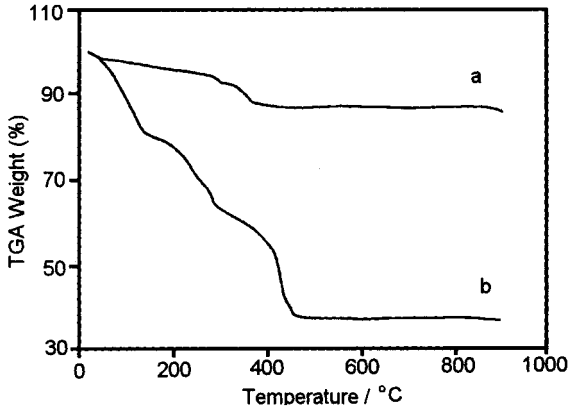


**Fig. 1** TGA curves of the two PMN precursors; (a) stepwise precipitation, (b) freeze-drying.

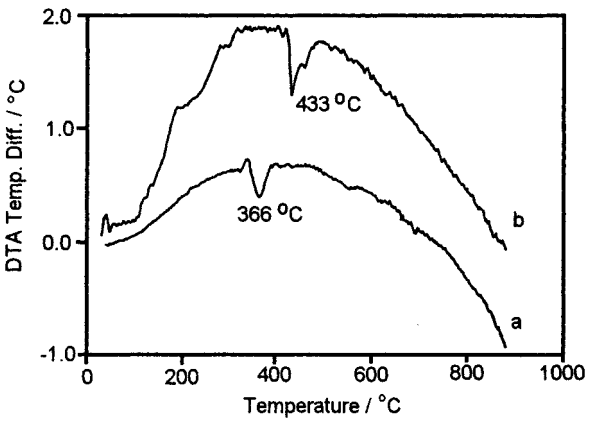


**Fig. 2** DTA curves of the two PMN precursors; (a) stepwise precipitation, (b) freeze-drying.

### Ceramic fabrication and characterization

The calcined powders were ball-milled using zirconia balls as the milling medium in ethanol for 48 hours to reduce particle agglomeration prior to being pressed into pellets of 10 mm in diameter. They were uniaxially pressed at a pressure of 100 MPa and then isostatically at a pressure of 345 MPa. Sintering of the pellets was carried out in covered high alumina crucibles at 1150 °C for 2 hours in air. The sintered pellets were characterized using XRD for phase analysis on sintered and polished surfaces. They were polished and coated with silver paint as electrodes and annealed at 700 °C for *ca.* 15 min. Dielectric measurements (relative permittivity and dissipation factor) were made using an LCR meter (HP 4284A) at three frequencies (1, 10, 100 kHz) as a function of temperature from −45–125 °C at a heating rate of 2 °C $min^{-1}$.

## Results and discussion

TGA and DTA results for the two PMN precursors are shown in Fig. 1 and 2, respectively. The stepwise precipitated precursor shows a steady weight loss with increasing temperature from room temperature to *ca.* 300 °C, where a minor fall in specimen weight occurs. This is followed by a major fall in specimen weight at 370 °C and a further small weight loss is observed at temperatures above 400 °C. In contrast, the freeze-dried precursor exhibits a much more drastic weight loss with increasing temperature from room temperature to *ca.* 430 °C, where there is a sharp fall in specimen weight. It also shows a much larger overall weight loss (*ca.* 64%) than that of the precipitated precursor (*ca.* 14%). This may easily be accounted for by the fact that the nitrate-based precursor is highly hygroscopic and is able to adsorb moisture quickly from the atmosphere.

Corresponding to the fall in specimen weight, the precipitated precursor demonstrates a broadened endotherm at 366 °C. This is related to the elimination of hydroxyl groups from the precursor as a result of decomposition of hydroxides. Similarly, the endotherm at 433 °C observed in the freeze-dried precursor is due to the decomposition of nitrates and the elimination of their residuals and water from the precursor. This is supported by the large fall in specimen weight at the same temperature. No noticeable DTA peaks are observed above 500 °C and the weight remains constant from 500 °C to *ca.* 850 °C when a slight drop in weight is observed for both samples. This could be attributed to the loss of lead by volatilization.

Fig. 3 and 4 show the XRD traces for the precursors derived *via* freeze-drying and stepwise precipitation, respectively, when calcined at various temperatures in the range from 700 °C to 1000 °C. The amount of perovskite phase present in each of the powders was estimated using the following equation as suggested by Swartz and Shrout,[30] on the basis of relative intensities of the major reflections for the pyrochlore and perovskite phases:

$$\text{Perovskite phase } \% = I_{PMN}/(I_{pyro} + I_{PMN}) \times 100$$

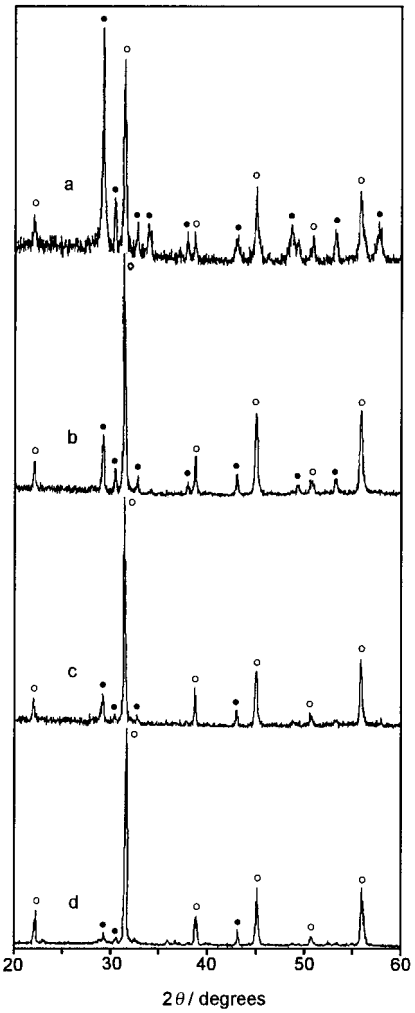


**Fig. 3** XRD patterns of the freeze-dried PMN powders calcined at (a) 700 °C, (b) 800 °C, (c) 900 °C and (d) 1000 °C, respectively. ○ and ● denote perovskite and pyrochlore phases respectively.

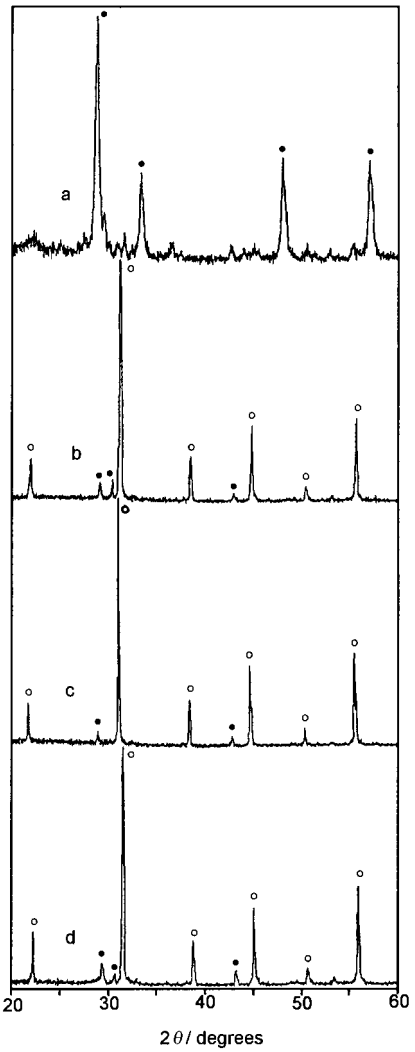


**Fig. 4** XRD patterns of the stepwise precipitated PMN powders calcined at (a) 700 °C, (b) 800 °C, (c) 900 °C and (d) 1000 °C respectively. ○ and ● denote perovskite and pyrochlore phases respectively.

**Table 1** Percentage of perovskite phase in the powders calcined at various temperatures

| Calcination temperature/°C | Freeze-drying (%) | Stepwise precipitation (%) |
|---|---|---|
| 700 | 47 | — |
| 800 | 81 | 95 |
| 900 | 89 | 97 |
| 1000 | 96 | 93 |

where $I_{PMN}$ refers to the intensity of the perovskite (110) peak and $I_{pyro}$ the intensity of the pyrochlore (222) peak. The percentages of perovskite phase present in the powders calcined at various temperatures are summarized in Table 1.

When calcined at 700 °C, the freeze-dried precursor exhibits *ca.* 47% perovskite phase. The amount of perovskite phase increases dramatically at the expense of the pyrochlore phase with increasing calcination temperature from 700–1000 °C. Only a trace amount of pyrochlore phase exists in the powder calcined at 1000 °C. A higher percentage of perovskite phase (*ca.* 80%) was obtained in the freeze-dried precursor prepared in the present work than in that prepared by Ho *et al.*,[27] who managed to obtain *ca.* 50% after calcination at 800 °C. Furthermore, much cheaper starting materials, such as niobium chloride, lead and magnesium nitrates, rather than ethoxides and acetates, have been used in the present work. As for the precipitated precursor, there is hardly any perovskite phase noticeable in the powder calcined at 700 °C. Perovskite PMN, however, becomes the predominant phase only when calcined at 800 °C. The percentage of perovskite phase (95%) formed at 800 °C is comparable to that obtained by Yoshikawa and Uchino[28] *via* a stepwise precipitation route using different starting materials. However, there is a slight decrease in the amount of perovskite phase formed in the precipitated powder calcined at 1000 °C when compared to that calcined at 900 °C. This is probably due to the excessive loss of lead oxide at high temperature as a result of the decomposition of PMN as described in the following equation:[19]

$$Pb(Mg_{1/3}Nb_{2/3})O_3 \rightarrow 1/6\ Pb_3Nb_4O_{13} + 1/2\ PbO + 1/3\ MgO$$

Research into the fabrication of PMN by the mixed oxide method has shown that pyrochlore phases are inevitably involved at the interface between PbO and $Nb_2O_5$ particles during the calcination process with the formation of the PMN perovskite phase at the junctions of PbO–MgO–$Nb_2O_5$ particles.[31] The transformation of the pyrochlore phase into the perovskite phase requires the diffusion of $Mg^{2+}$ ions. In the freeze-drying process, chemical homogeneity of the precursor is preserved since little atomic movement is possible during the low-temperature sublimation.[32] Hence the formation of perovskite PMN is easily accomplished in the freeze-dried precursor as long distance diffusion of cations is not required. In the stepwise precipitated precursor, however, the distribution uniformity of cations is not as good since magnesium hydroxide was precipitated separately at the second stage of precipitation. This could explain the formation of perovskite PMN at 700 °C in the freeze-dried precursor, and why the precipitated precursor requires a temperature of 800 °C.

Fig. 5 and 6 show the agglomerate size distributions of the PMN powders derived *via* the two processing routes, when

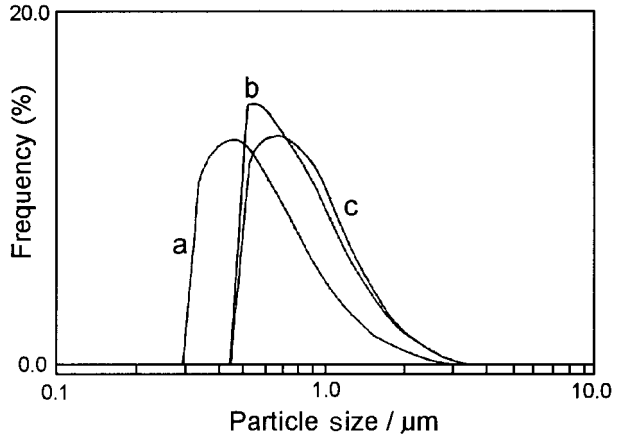


**Fig. 5** The particle size distribution of the freeze-dried powder calcined at (a) 800 °C, (b) 900 °C and (c) 1000 °C.

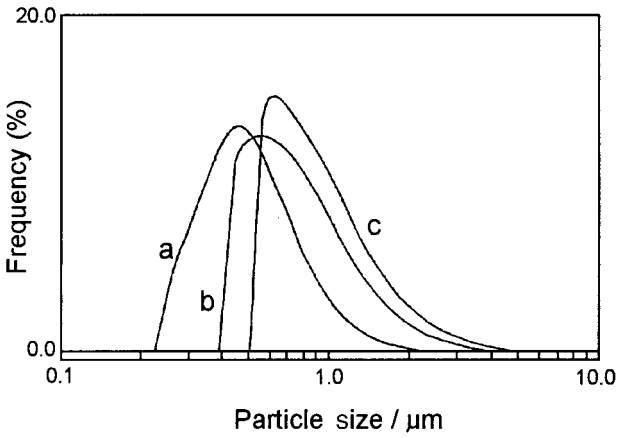


**Fig. 6** Particle size particle distribution of the stepwise precipitated powder calcined at (a) 800 °C, (b) 900 °C and (c) 1000 °C.

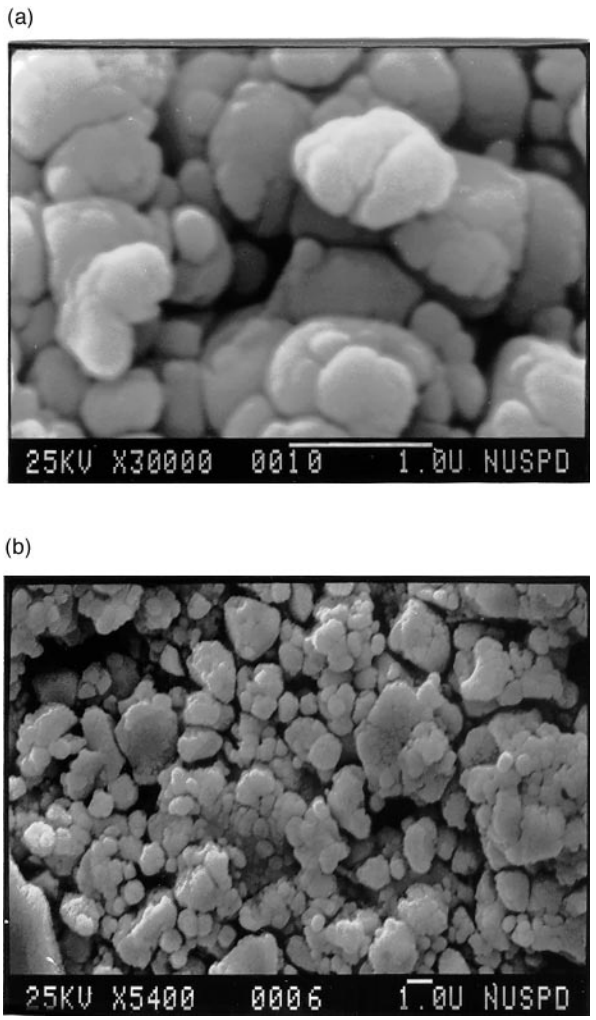


**Fig. 7** SEM micrographs (a) of the freeze-dried powder calcined at 900 °C and (b) of the stepwise precipitated powder calcined at 900 °C.

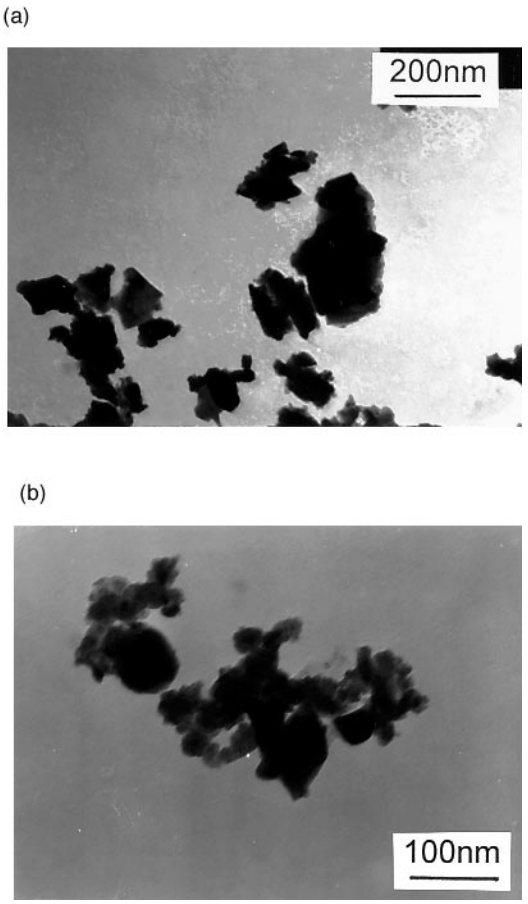


**Fig. 8** TEM micrographs (a) of the freeze-dried powder calcined at 900 °C and (b) of the stepwise precipitated powder calcined at 900 °C.

calcined at 800, 900 and 1000 °C. All these powders show an average agglomerate size of less than 1.0 μm although they cover a size range from submicrons to *ca.* 5 μm. As expected, they demonstrate an increase in average agglomerate size with increasing calcination temperature. As evidenced from the micrographs shown in Fig. 7(a, b), for the powders calcined at 900 °C, both PMN powders exhibit a rounded morphology and they form agglomerates of *ca.* 1 to 5 μm in size. The primary particles in the agglomerates are, however, submicrometric in size. This is confirmed by the TEM micrographs shown in Fig. 8(a, b) for the powders calcined at the same temperature. Table 2 summarizes the average agglomerate sizes in the two powders when calcined at 800, 900 and 1000 °C.

The powders calcined at 900 °C obtained *via* the two processes were pressed into pellets and sintered at 1150 °C in air for 2 h. XRD profiles for the sintered PMN ceramics produced by freeze-drying and stepwise precipitation are illustrated in Fig. 9 and 10, respectively. The pyrochlore phase was found to exist in the precipitated PMN on both the sintered and the polished surfaces. The increased amount of pyrochlore phase in the sintered PMN when compared to that present in the calcined powders is due to the further loss of lead oxide at the high sintering temperature. On the other hand, the freeze-dried PMN shows a pure perovskite phase on both

**Table 2** Average agglomerate sizes of the powders calcined at various temperatures

| Calcination temperature/°C | Freeze-drying/μm | Stepwise precipitation/μm |
|---|---|---|
| 800 | 0.417 | 0.417 |
| 900 | 0.510 | 0.544 |
| 1000 | 0.624 | 0.583 |

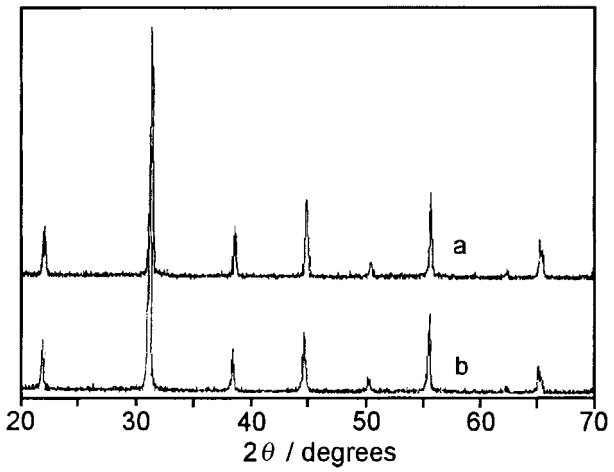


**Fig. 9** XRD traces of the (a) sintered and (b) polished surfaces of freeze-dried PMN pellet sintered at 1150 °C.

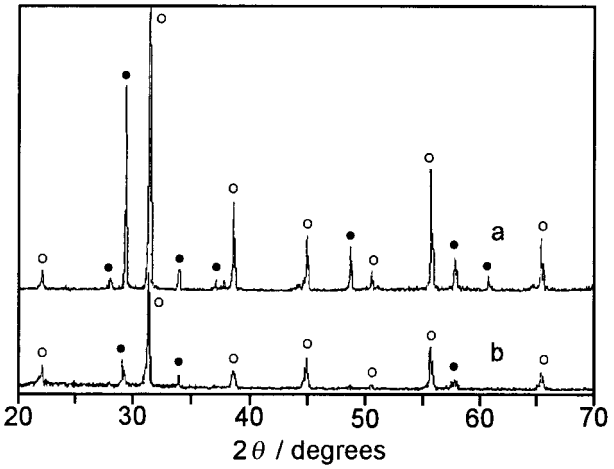


**Fig. 10** XRD traces of the (a) sintered and (b) polished surfaces of stepwise precipitated PMN pellet sintered at 1150 °C (○ and ● denote perovskite and pyrochlore phases respectively).

sintered and polished surfaces despite the presence of a minimal amount of pyrochlore phase in the calcined powders. Hence, the pyrochlore phase has been eliminated at the sintering temperature. Similar observations were reported by Ho *et al.*,[27] who carried out freeze-drying on an alkoxide solution.

Dielectric properties of the sintered PMN are shown in Fig. 11 and 12 for the materials derived from freeze-drying

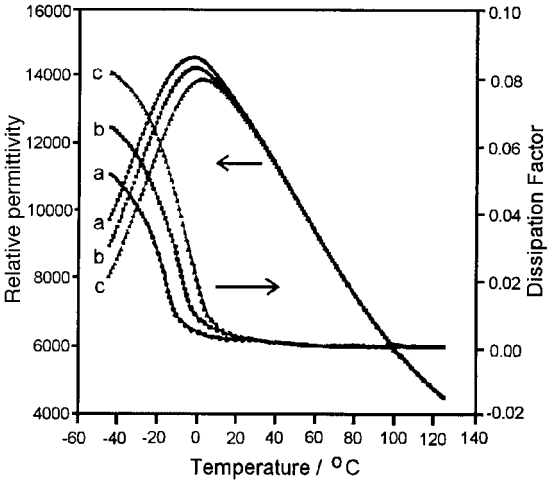


**Fig. 11** Dielectric properties of the freeze-dried PMN sintered at 1150 °C; (a) 1 kHz, (b) 10 kHz, (c) 100 kHz.

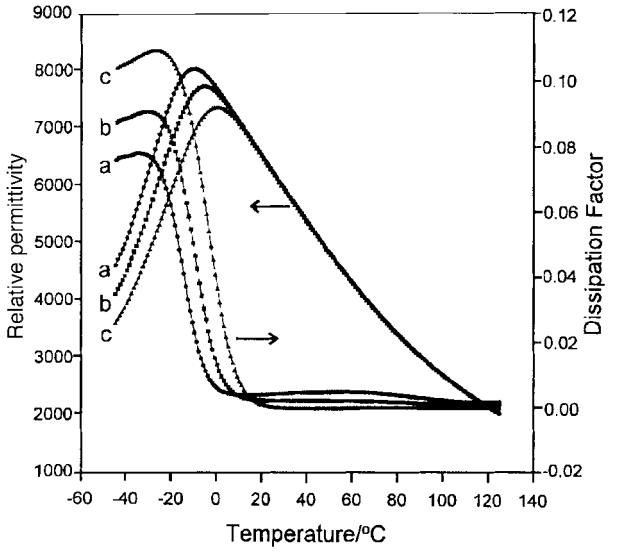


**Fig. 12** Dielectric properties of the stepwise precipitated PMN sintered at 1150 °C; (a) 1 kHz, (b) 10 kHz, (c) 100 kHz.

**Table 3** Dielectric properties of PMN sintered at 1150 °C

| Processing route | Frequency/kHz | $T_c$/°C | $\varepsilon_{max}$ | $\varepsilon_{25}$ |
|---|---|---|---|---|
| Freeze-drying | 1 | −3 | 14542 | 12678 |
| | 10 | −2 | 14232 | 12586 |
| | 100 | 1 | 13896 | 12554 |
| Stepwise precipitation | 1 | −11 | 8019 | 6914 |
| | 10 | −6 | 7711 | 6174 |
| | 100 | −1 | 7344 | 6161 |

and stepwise precipitation, respectively. Table 3 is a summary of Curie temperature $T_c$, maximum relative permittivity $\varepsilon_{max}$ and room temperature relative permittivity $\varepsilon_{25}$ at various frequencies. Typical relaxor behaviour of decreasing maximum relative permittivity with an increase in Curie temperature upon raising the frequency is observed for both PMN pellets. However due to the presence of pyrochlore phase as observed in Fig. 10, the relative permittivity of the precipitated PMN is much lower than that of the freeze-dried PMN. The former reaches a maximum of 8019 with a Curie temperature of −11 °C at 1 kHz while the latter shows a maximum relative permittivity of 14542 and a Curie temperature of −3 °C at the same frequency. A smaller dissipation factor (<0.09) at all frequencies is also obtained for the freeze-dried PMN in comparison to that of the precipitated PMN.

## Conclusions

PMN powders with less than 5% pyrochlore phase have been successfully prepared *via* two chemistry-based processing routes, namely stepwise precipitation and freeze-drying, from an aqueous Pb–Mg–Nb nitrate solution. The precursor derived from stepwise precipitation forms PMN of 97% perovskite phase when calcined at 900 °C and the freeze-dried derived precursor forms 96% perovskite phase at 1000 °C. Both PMN powders exhibit a rounded agglomerate morphology and an average agglomerate size of <1.0 μm. PMN ceramics of pure perovskite phase can be obtained when the freeze-drying derived powder is sintered at 1150 °C while the pyrochlore phase persists in the PMN ceramics derived from stepwise precipitation. Therefore the freeze-dried PMN shows a higher maximum relative permittivity (14542) than that of precipitated PMN which exhibits a maximum relative permittivity of 8019 at 1 kHz frequency.

The authors would like to thank Madam G. L. Loy of the School of Biological Science, Y. F. Looy and G. K. Lim for their help in taking the transmission electron micrographs. We are also grateful to Dr J. M. Xue and D. M. Wan for their help and discussions throughout the course of this project.

## References

1 S. L. Swartz, T. R. Shrout, W. A. Schulze and L. E. Cross, *J. Am. Ceram. Soc.*, 1984, **67**, 311.
2 V. A. Bokov and I. Emyl'Nikova, *Sov. Phys. Solid State*, 1961, **2**, 2438.
3 G. A. Smolenskii and A. I. Agranovskaya, *Sov. Phys. Solid State*, 1960, **1**, 1429.
4 S. L. Jang, K. Uchino, S. Nomura and L. E. Cross, *Ferroelectrics*, 1980, **27**, 31.
5 L. E. Cross, S. J. Jang, R. E. Newnham, S. Nomura and K. Uchino, *Ferroelectrics*, 1980, **23**, 187.
6 K. Uchino, S. Nomura, L. E. Cross, S. J. Jang and R. E. Newnham, *J. Appl. Phys.*, 1980, **51**, 1142.
7 S. Nomura and K. Uchino, *Ferroelectrics*, 1982, **41**, 117.
8 D. K. Agrawal, R. Roy and H. A. Mckinstry, *Mater. Res. Bull.*, 1987, **22**, 83.
9 L. A. Shebanov, P. P. Kapostins and J. A. Zvirgzds, *Ferroelectrics*, 1984, **56**, 53.
10 C. N. R. Rao, *Mater. Sci. Eng. B: Solid State Mater.*, 1993, **18**, 1.
11 A. Watanabe, H. Haneda, Y. Mosiyoshi, S. Shirasaki, S. Kuramoto and A. Yamamura, *J. Mater. Sci.*, 1997, **27**, 1245.
12 H. U. Anderson, M. J. Pennell and J. P. Guha, *Adv. Ceram. Mater.*, 1987, **21**, 91.
13 T. Fukui, C. Sakurai and M. Okuyama, *J. Non-Cryst. Solids*, 1991, **134**, 293.
14 P. Ravindranathan, S. Komarneni, A. S. Bhalla, R. Roy and L. E. Cross, *Ceram. Trans.*, 1988, **1**, 182.
15 J. H. Choy, J. S. Yoo, S. G. Kang, S. T. Hong and D. G. Kim, *Mater. Res. Bull.*, 1990, **25**, 283.
16 S. A. Costantino, G. O. Dayton and J. V. Biggers, *Ceram. Trans.*, 1990, **8**, 123.
17 K. Katayama, M. Abe and T. Akiba, *Ceram. Int.*, 1989, **15**, 289.
18 S. M. Gupta and A. R. Kulkarni, *Mater. Res. Bull.*, 1993, **28**, 1295.
19 S. M. Gupta and A. R. Kulkarni, *J. Eur. Ceram. Soc.*, 1996, **16**, 473.
20 R. E. Riman, in *Colloid and Surface Engineering: applications in the process industries*, ed. R. A. Williams, Butterworth-Heinemann, Oxford, 1992, p. 140.
21 C. Lacour, F. Laher-Lacour, A. Dubon, M. Lagues and P. Mocaer, *Physica C*, 1990, **167**, 287.
22 F. J. Schnettler, F. R. Monforte and W. W. Rhodes, *Sci. Ceram.*, 1968, **4**, 79.
23 E. Bermejo, T. Dantas, C. Lacour and M. Quarton, *Mater. Res. Bull.*, 1995, **30**, 5, 645.
24 E. Bermejo, M. Quarton and C. Lacour, *Mater. Res. Bull.*, 1994, **29**, 965.
25 T. Tachiwaki, M. Suzuki, H. Okajima, S. Koizumi, T. Ito and A. Hiraki, *Appl. Surf. Sci.*, 1993, **70/71**, 751.
26 M. A. Akbas and W. E. Lee, *J. Eur. Ceram. Soc.*, 1995, **15**, 57.
27 J. C. Ho, K. S. Liu and I. Nankin, *J. Mater. Sci.*, 1995, **30**, 3936.
28 Y. Yoshikawa and K. Uchino, *J. Am. Ceram. Soc.*, 1996, **79**, 2417.
29 J. W. Mellor, in *A Comprehensive Treatise on Inorganic and Theoretical Chemistry*, Longmans, London, 1964, vol. 9, p. 861.
30 S. L. Swartz and T. R. Shrout, *Mater. Res. Bull.*, 1982, **17**, 1245.
31 T. R. Shrout and A. Halliyal, *Am. Ceram. Soc. Bull.*, 1987, **66**, 704.
32 S. H. Gelles and F. K. Roehrig, *J. Met.*, 1972, June, 23.

*Paper 8/04428G*